Environmental Science & Technology

pubs.acs.org/est

Article

Frozen Hydrogen Peroxide and Nitrite Solution: The Acceleration of Benzoic Acid Oxidation via the Decreased pH in Ice

Yong-Yoon Ahn, Jungwon Kim, and Kitae Kim*

Cite This: *Environ. Sci. Technol.* 2022, 56, 2323−2333

Read Online

ACCESS | Metrics & More | Article Recommendations | Supporting Information

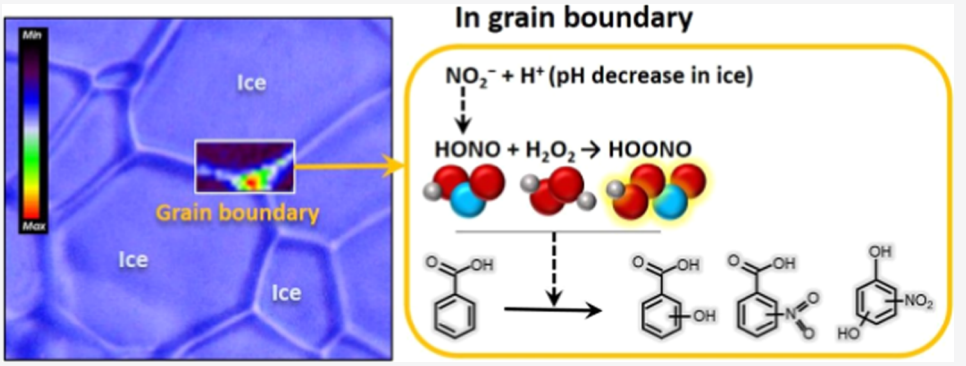

ABSTRACT: We investigated benzoic acid oxidation via the reaction of hydrogen peroxide (H_2O_2) and nitrite (NO_2^-). The oxidation of benzoic acid by reactive nitrous acid (HONO) was negligible, and the reactivity of the H_2O_2/NO_2^- system decreased with a decrease in temperature under aqueous conditions. However, freezing markedly accelerated the chemical reaction. Based on Raman microscope measurements, concentrated species were confirmed in certain regions of the ice. We proposed that the change in nitrite speciation (accordingly, a decrease in the pH below pK_a), derived from the freezing concentration effect, was the reason for the accelerated reactions. The oxidation characteristics of the system were monitored under varying conditions, such as initial pH, dosage ratio, benzoic acid concentration, and reaction with various benzene derivatives. The ultrahigh-performance liquid chromatography/electrospray ionization/mass spectrometry (UHPLC/ESI/MS) measurement showed that peroxynitrous acid (HOONO)-mediated oxidation generated hydroxylated and nitrated byproducts. Additionally, decarboxylated products were detected, indicating direct electron transfer from the organic compounds to HOONO. As freezing is a global phenomenon, and H_2O_2 and NO_2^- are ubiquitous in the environment, the transformation of aromatic compounds with H_2O_2/NO_2^- in cold environments must be considered in environmental chemistry.

KEYWORDS: *ice, peroxynitrous acid, benzoic acid, nitrous acid, freeze concentration*

INTRODUCTION

The environmental chemistry of aromatic substances is of great importance because they influence Earth's carbon cycle.[1−6] Among the variety of species associated with hydrocarbon transformation, nitrite has been intensively highlighted owing to its importance in photochemistry as a source of nitric oxide and hydroxyl radicals, as well as its inherent reactivity when protonated to form nitrous acid.[4−11] Generally, most studies on nitrite chemistry have focused on aqueous and gaseous phase reactions. However, its unique behavior during freezing has also been identified and analyzed.[12−14] This unique behavior is the significant acceleration of the reaction during freezing compared with the liquid phase when the pH is ∼4.[15,16]

This freezing-induced acceleration is mostly caused by the freeze concentration effect, which refers to the accumulation of dissolved species in the liquid-like layer of ice (or the ice grain boundary).[15] However, Takenaka et al.[13] inferred that the reaction involving nitrite during freezing cannot be interpreted solely based on the freeze concentration effect; the speciation of nitrite to nitrous acid must be considered. Although the substances concentrated at the ice grain boundaries, the nitrite reactivity during freezing was inert under circumneutral and alkaline pH conditions.[15,16] Additionally, many studies have reproduced the phenomenon of a 2- to 4-fold decrease in the pH in the liquidlike region of ice when the pH before freezing was slightly acidic; these studies have proposed that proton accumulation and cation−anion separation at the ice grain

Received: August 24, 2021
Revised: November 24, 2021
Accepted: November 30, 2021
Published: December 14, 2021

boundary and ice-bulk were mainly responsible for this phenomenon.[17−23] Accordingly, in this acidic environment in ice, nitrite can transform to reactive nitrous acid (HONO; pK_a = 3.4) and the nitrous acidium ion (H_2ONO^+; pK_a = 1.7),[24] despite a circumneutral pH before freezing. These substances can react with aromatic compounds, such as guaiacol,[6] methylcatechol,[5] acetaminophen,[25] and phenol[3,26] to generate nitrated aromatic compounds, which have an important role in environmental chemistry.

In addition to the reaction of nitrous acid, enhanced phenol nitration has been reported, which was caused via the introduction of hydrogen peroxide into a nitrite solution.[3] Previous studies have shown that nitrite does not react with hydrogen peroxide at an appreciable rate, but nitrous acid reacts rapidly with hydrogen peroxide and transforms into peroxynitrous acid (HOONO), which is responsible for the accelerated nitrophenol generation. Although the reaction mechanism of HOONO is not yet fully understood, its reactivity has been ascribed to (i) one- or two-electron transfer oxidation, (ii) the generation of NO_2^+ ion from the heterolytic cleavage of the peroxo O−O bond, or (iii) the formation of a $[^{\bullet}NO_2 + {}^{\bullet}OH]_{cage}$ caged radical pair or its individual free radicals through the homolytic cleavage of the peroxo O−O bond.[27−34] Hence, HOONO behaves not only as a nitration reagent but also as a hydroxylation reagent.[35] Numerous studies have discussed the reactions with HOONO with respect to the generation of $^{\bullet}OH$ based on the apparent observation of hydroxylated byproducts;[28,34,36,37] other studies have also proposed that $^{\bullet}OH$ cannot be generated from the homolysis of HOONO.[30,38,39] Owing to its complex chemistry, these controversies have not been resolved until now. However, regardless of the detailed reaction mechanism, HOONO can be regarded as a sufficiently strong oxidant, which reacts nonselectively with various organic compounds in the environment, as well as $^{\bullet}OH$.

In this study, we propose a novel chemical reaction mechanism, i.e., the accelerated oxidation of aromatic substances in the frozen hydrogen peroxide and nitrite solution. We tested the oxidation of benzoic acid (BA) as a representative aromatic compound because its structure is ubiquitous in various organic compounds in the environment[1] and drugs,[40] and it resists the oxidative attack of HONO, as shown in our experiment. This negligible reactivity is important because many studies on aromatic nitration have discussed nitration-prone compounds, such as phenol, to analyze the role of nitrous acid.[3,5,6,27,28] However, we also need to consider nitration-resistant compounds under certain conditions. Furthermore, low temperatures inhibit aromatic nitration[4] such that freezing-accelerated BA transformation can provide new HOONO-mediated pathways in environmental chemistry. Accordingly, we compared the transformation efficiency of BA in aqueous and frozen systems. We attempted to reveal the reason for accelerated BA oxidation in the frozen system, which is related to the acid dissociation constant of nitrite and the acidity in the ice. We confirmed the freeze concentration in the ice. We then tested the influence of the stoichiometric ratio between the reactants. The substrate-dependent reactivity of the system was also investigated. The reaction byproducts were detected to understand the characteristics of oxidation. The system was also investigated under imitated natural conditions, i.e., water environments (stream or rain) and freezing conditions (ethanol bath or air-cooling). Water freezing commonly occurs in the upper atmosphere, polar regions, and middle latitude in winter. Hydrogen peroxide and nitrite are present in water droplets, haze, rain, and surface water, among others, which can be frozen. Based on these circumstances, our study demonstrates the important role of freezing in the transformation of organic compounds in the environment.

EXPERIMENTAL SECTION

Chemicals. The chemical reagents used in this study are listed in the Supporting Information (Text S1). All chemicals were of reagent grade and were used as received without any further purification. The entire chemical solutions used in this study were prepared with ultrapure deionized water (18.2 MΩ·cm), which was produced by a Milli-Q Water Purification System (Millipore). The natural waters (i.e., rain and stream) were obtained as follows: We gathered rainwater at the rooftop of the KOPRI building from September 28−29, 2021. We collected stream water from the Seongbuk stream, Korea, on October 6, 2021. All collected natural waters were filtered using a 0.2 μm PTFE filter and stored in a refrigerator.

Experimental Procedure. The test solution was prepared in a 100 mL glass beaker. H_2O_2 (100 mM), $NaNO_2$, and BA stock solutions (10 mM) were appropriately added to the beaker to obtain the desired concentration. Then, $HClO_4$ solutions were added to obtain the initial pH value. Next, 10 mL of this solution was poured into a 15 mL polypropylene conical tube sealed with a cap. The conical tube containing the test solution was placed in an ethanol-cooling bath, which was precooled to desired temperatures (−20, −10, 5, 15, 25, and 35 °C). The number of conical tubes was selected according to the time-sampling points. These preparation procedures were conducted as fast as possible (~30 s was required), and we assigned the moment at which the conical tubes were immersed in the cooling bath as the starting point (i.e., t = 0). The frozen conical tube was withdrawn from the cooling bath at a particular time and then placed in a lukewarm water bath at 30 °C to thaw the ice for chemical analysis. Note that the influence of thawing in 30 °C within 10 min is negligible as presented in Figure 1 (see 35 °C in Figure 1). After thawing, the samples were analyzed immediately. At least two runs of each experiment were performed to confirm the data reproducibility. When we needed to freeze the solution using the air-cooling system, the conical tubes were placed in a custom-made low-temperature chamber, which operated at −20 °C with marginal temperature variation from the programmed value.

Analytical Methods. High-pressure liquid chromatography (HPLC) (Agilent, 1260 Infinity II) was employed to analyze the organic compounds in this study. The organic compounds are identified by examining retention time (Poroshell 120 EC-C18 column (4.6 mm × 150 mm) was used) and absorbance (using a variable-wavelength detector (G7114 1260VWD)). In the analysis, 0.1% (v/v) phosphoric acid and acetonitrile were used as eluents, and the composition ratio between them varied according to the target organic compound.

The nitrite and nitrate concentrations were measured using an ion chromatograph (Dionex ICS-1100) with a suppressor (Dionex AERS 500), column (Dionex IonPac AS23), and conductivity detector. Sodium carbonate and bicarbonate solution (0.477 and 0.067 g in 1 L, respectively) were used for elution.

https://doi.org/10.1021/acs.est.1c05705
Environ. Sci. Technol. 2022, 56, 2323−2333

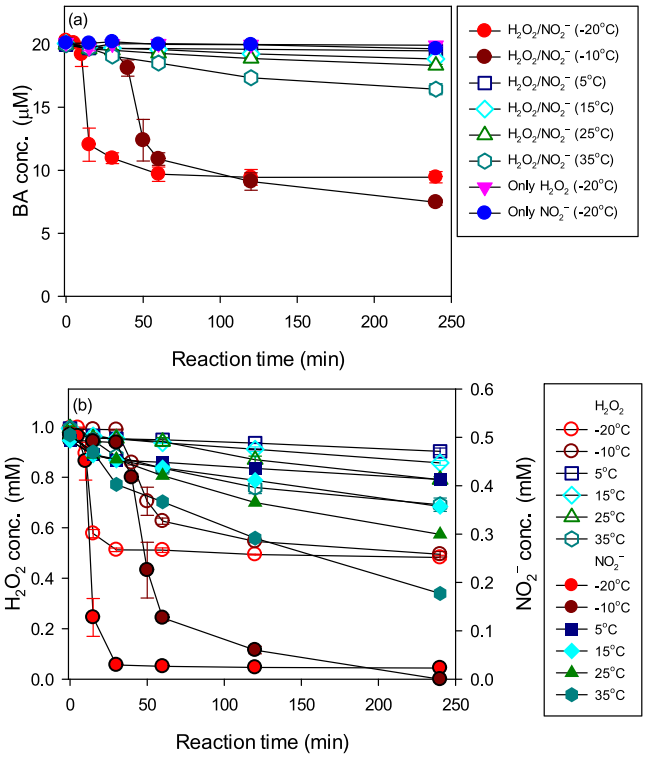

Figure 1. Time profiles of substrate concentrations in the H_2O_2/NO_2^- system. (a) Concentration of BA. (b) Concentrations of H_2O_2 and NO_2^-. Experimental conditions: $[BA]_0$ = 20 μM; $[H_2O_2]_0$ = 1 mM; $[NO_2^-]_0$ = 0.5 mM; pH_i = 4.0 (adjusted by $HClO_4$).

The H_2O_2 concentration was measured via the modified iodometry method, as described in Klassen et al.[41] Specifically, 0.05 mL of sample was mixed with 2.85 mL of 10 mM KI (in 10 mM $NaHCO_3$) and 0.1 mL of 10 mM ammonium molybdate (total volume of 3 mL); this solution was incubated in the atmosphere for 1 h. The absorbance at a wavelength of 352 nm was monitored to calibrate H_2O_2 concentration. We confirmed that other oxidants, such as HONO, did not interfere with the signal, and was well reproduced at various H_2O_2 concentration standards. UV−vis spectroscopy was used to monitor the H_2O_2 concentration with a UV-2600i (Shimadzu).

A confocal Raman microscope (Renishaw, InVia Qontor) was employed to obtain information on the reagent distribution in the ice without melting. A temperature-controlled microscope stage (Linkam Scientific, THMS600) was used to freeze the sample with a cooling speed of −2 °C/min and a terminal temperature of −20 °C. The 532 nm laser was exposed for 1 s with data accumulation 10 times, and the laser power on the spot was less than 1.5 mW.

The oxidation byproducts were analyzed using a UHPLC (Thermo Fisher Scientific, Vanquish) combined with a quadrupole-orbitrap mass spectrometer (Thermo Fisher Scientific, Q Exactive Focus). The separation was performed on a Hypersil GOLD aQ column with a mobile phase composed of 0.1% (v/v) formic acid (dissolved in LC-MS grade water) and neat acetonitrile (LC-MS grade) at a flow rate of 0.3 mL/min. Mass detection was carried out in negative electrospray ionization (ESI) mode, and the operating parameters were set as follows: a detection range of 50−550 m/z, with a resolution of 70 000, spray voltage of 4.00 kV, capillary temperature of 320 °C, sheath gas flow rate of 40 au, auxiliary gas flow rate of 10 au, auxiliary gas heater temperature of 300 °C, S lens RF level of 50.0, maximum injection time of 200 ms, and automatic gain control (AGC) target of 1×10^6. The obtained total ion current (TIC) signals were analyzed using the Compound Discoverer 3.2 (Thermo Fisher Scientific) software with Chemspider and mzCloud database to identify and confirm the detected byproducts. Total organic carbon (TOC) was measured using a TOC Analyzer (TOC-LCPH, Shimadzu).

RESULTS AND DISCUSSION

Freezing-Induced Enhancement of Reaction between Hydrogen Peroxide and Nitrite. Figure 1a shows the degradation of BA in the H_2O_2/NO_2^- system at a pH of 4. In the aqueous cases (i.e., the temperature was >0 °C), the decrease in BA did not exceed 20% of its initial concentration during the reaction. However, when the solution was frozen (i.e., the temperature was −20 and −10 °C), approximately half of the initial BA decomposed. The degradation of BA during freezing was not observed when H_2O_2 or NO_2^- was absent from the solution (Figure 1a; pink triangle and blue circle). Similarly, the concentrations of H_2O_2 and NO_2^- changed rapidly when the solution was frozen, whereas they gradually decreased when the solution was not frozen (Figure 1b). It is noteworthy that the initiation of freezing at −10 °C required ∼30 min, and the concentration change within that period was very little, but the remarkable change of concentration occurred after that period. Also, we emphasize that the concentration changes in the aqueous conditions were reduced with a decrease in the temperature. However, when the solution was frozen, the reaction between the reagents increased, and most of the NO_2^- was converted to NO_3^- (Figure S1). We note that although the only presence of NO_2^- also showed a change in its concentration due to freezing, the rate was significantly lower than that in the case of its coexistence with H_2O_2 (Figure S1). Based on these observations, we concluded that H_2O_2 and NO_2^- are essential for initiating BA degradation, and the reactions between them increased as a result of freezing. We also point out that ∼20% of the total nitrite concentration occurred in a protonated form at a pH of 4, i.e., nitrous acid (Figure S2).[24] As a reactive nitrogen species, HONO can transform various aromatic compounds, including phenol, catechol, acetaminophen, aniline, and benzene.[2,25,26,42] Additionally, Sun et al.[43] reported that freezing can accelerate sulfamethoxazole transformation by nitrite at circumneutral pH values. However, we found no BA decomposition by NO_2^- at a pH of 2−5 (note that, at a maximum, 80% of the NO_2^- existed as HONO; Figure S2) in both the aqueous and frozen systems (Figure S3a). We expect that the negligible reactivity of HONO toward BA derives from the function of the electron-withdrawing carboxyl group, which resists the electrophilic substitution of HONO (or NO^+) on the aromatic ring of BA.[44] Thus, we inferred that the BA decomposition originated from the action of other reactive species, derived from the reaction between H_2O_2 and nitrite species (i.e., HONO and NO_2^-). According to previous studies, the reaction between H_2O_2 and NO_2^- generates reactive peroxynitrous acid (HOONO) as follows[3,45,46]

$$H_2O_2 + HONO \rightarrow HOONO + H_2O \quad (1)$$

$$HOONO \leftrightarrow OONO^- + H^+ (pK_a = 6.8) \quad (2)$$

https://doi.org/10.1021/acs.est.1c05705
Environ. Sci. Technol. 2022, 56, 2323−2333

$$HOONO \rightarrow NO_3^- + H^+(\text{isomerization}) \quad (3)$$

$$HOONO \rightarrow NO_2^+ + OH^-(\text{heterolytic cleavage}) \quad (4)$$

$$HOONO \leftrightarrow [^{\bullet}NO_2 + {}^{\bullet}OH]_{cage} \quad (5)$$

The pK_a of $ONOO^-$ is 6.8; thus, it occurs as a protonated species under acidic condition.[27] In the previous research, the activation energy of forming NO_2^+ and HNO_3 from the reaction of H_2O_2 and HNO_2 at pH 4.5 were calculated as 94 ± 8 and 75 ± 35 kJ/mol, respectively.[4] We noted that, under aqueous conditions at a pH of 4, we obtained the activation energy of NO_2^- transformation of 38.56 ± 3.27 kJ/mol from the plot of the Arrhenius relationship (Figure S4).

The decomposition of BA is sensitive to pH. Figure 2a illustrates the pH dependence of BA degradation in the H_2O_2/NO_2^- system. We found that ∼65% of the BA decomposed at a pH of 3, even under aqueous conditions, but freezing accelerated this reaction (note that the absence of NO_2^- resulted in no degradation of BA; Figure S3b). Overall, the BA degradation efficiency decreased with an increase in the pH. Furthermore, no changes were observed at a pH of 5, regardless of freezing. As the pK_a of nitrite is 3.4 ($HNO_2 \leftrightarrow NO_2^-$),[3,10,24] it is plausible that oxidant generation, which is responsible for BA degradation, is highly related to nitrite speciation. As demonstrated in previous studies, the NO_2^- disappearance rate by H_2O_2 is significantly related to the pH and pK_a values of the reactants.[3] This reaction eventually produces HOONO, but HOONO is rapidly decomposed and isomerized to a relatively stable form: nitrate (NO_3^-).[27] Accordingly, we found a positive relationship between the decomposition of BA and the conversion of NO_2^- to NO_3^- by H_2O_2 (see the aqueous cases in Figure 2). In addition, the molar ratio of the reaction between H_2O_2 and NO_2^- is likely 1:1 because we observed that ∼0.45 mM of NO_3^- was generated from the reaction of 1 mM H_2O_2 and 0.5 mM NO_2^- (an ∼90% conversion from NO_2^-), with a remainder of ∼0.5 mM H_2O_2 (Figure 2b). Note that the effect of NO_3^- on the system was negligible because the transformation of BA by 0.5 mM NO_3^- with and without H_2O_2 at a pH of 3 was ineffective, although nitric acid is a strong nitration reagent (the pK_a of HNO_3 is <−1 such that it had likely fully dissociated and had no oxidative effect under our experimental condition; Figure S5). Furthermore, the oxidation of BA is likely caused by short-lived substances because we found that only less than 5 μM BA decomposition when BA was added later into the H_2O_2/NO_2^- solution, which proceeded during the reaction between them (Figure S6). Thus, considering HOONO as the main oxidant is reasonable.

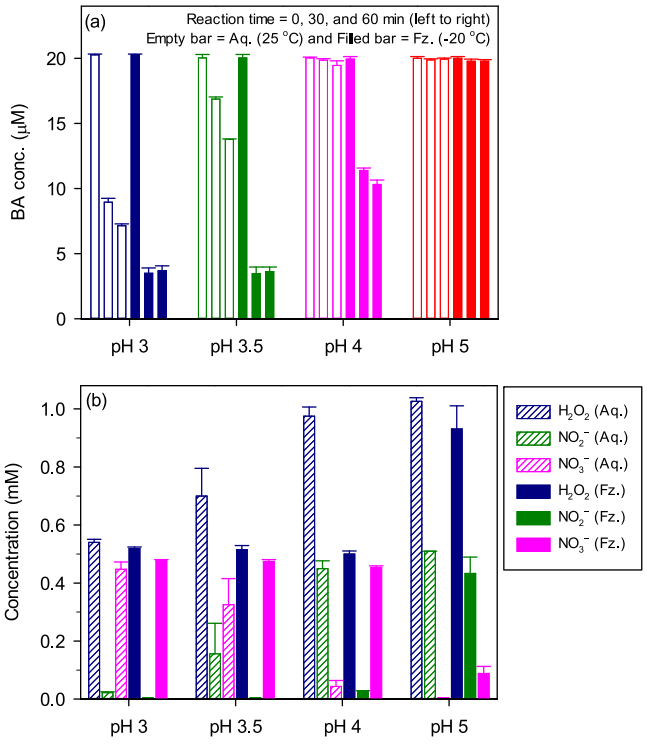

Figure 2. Effect of pH on the H_2O_2/NO_2^- system. (a) Concentration of BA. (b) Concentration of H_2O_2, NO_2^-, and NO_3^-. Experimental conditions: $[BA]_0$ = 20 μM; $[H_2O_2]_0$ = 1 mM; $[NO_2^-]_0$ = 0.5 mM; temperature: frozen system (Fz.) = −20 °C, aqueous system (Aq.) = 25 °C; reaction time = 1 h.

As shown in Figure 2, the reactivity of the system increased as pH decreased. Hence, the accelerated BA decomposition in ice can be interpreted as a freezing-induced decrease in the pH. It is remarkable that a slight generation of NO_3^- was found at pH 5 under the frozen condition while no conversion to NO_3^- was detected under aqueous conditions (Figure 2b). Owing to the freeze concentration effect, the liquidlike layer in the ice grain boundary can become more acidic via the freezing of an acidic solution.[15] According to studies on dichromate reduction in ice, freezing-induced changes in the pH change influence the reactivity of Cr species (roughly, pH 4 to 1) because the Cr(VI) species can be affected by the proton concentration and, consequently, its thermodynamic relationship in the system.[47−49] Similarly, during freezing, the speciation of NO_2^- changes to more reactive HONO and its reactivity with H_2O_2 increased. To verify the pH drop phenomenon during freezing, it was visualized using cresol red (CR), which was employed as a pH indicator in the ice sample (Figure 3a). The color change in CR occurs if the pH of the system changes from 4 to near 1.1 due to the pK_a of CR.[15] As shown in the inset of Figure 3a, the light yellow color of the sample changed to light pink when the sample was completely frozen. In addition, the peak position of absorbance of the sample was found at 434 and 520 nm for the original and frozen samples, respectively, which are consistent with the reported values of the monoprotonated and diprotonated form of CR.[50] According to the Henderson−Hasselbalch equation, we assumed that the pH of the ice was <1.435 (see Text S2 for a detailed description). However, we need to mention that the current level of understanding in thermodynamics in ice, such as an equilibrium constant at a liquidlike region, is very limited, but these issues are beyond the scope of the present study.[51,52]

Figure 3b shows the freeze concentration effect at the ice grain boundary. The color in the center box represents the Raman signal intensity at this position (note that red and violet-black indicate high and low intensity, respectively). The Raman peaks for H_2O_2, NO_2^-, and BA well agreed with the literature.[53−55] As demonstrated, high signals occurred at the interfacial and vertex positions of the ice grains. This result indicates that the dissolved reagents apparently accumulated in a specific area (i.e., the ice grain boundary or micro pocket) in the ice. When we mixed all of the reagents comprising the H_2O_2/NO_2^- system, we only found a weak peak at 877 cm^{-1} (O−O stretching of H_2O_2) and a strong peak at 1050 cm^{-1} (NO_3 in-phase symmetric stretching) in the scanned area due

https://doi.org/10.1021/acs.est.1c05705
Environ. Sci. Technol. 2022, 56, 2323−2333

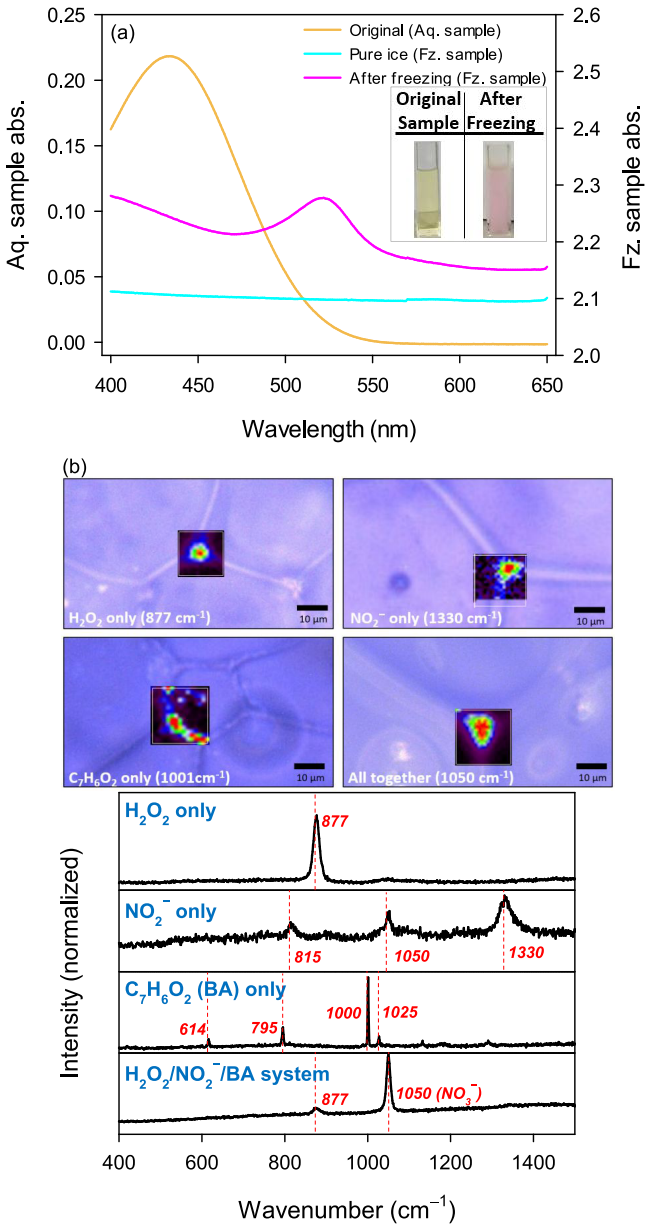

Figure 3. (a) UV−visible absorption spectra of CR. Insert = color of cresol red. Experimental conditions: $[CR]_0$ = 10 μM; $[H_2O_2]_0$ = 1 mM; $[NO_2^-]_0$ = 0.5 mM; pH_i = 4.0 (adjusted by $HClO_4$); temperature: frozen system (Fz.) = −20 °C; aqueous system (Aq.) = 25 °C. (b) Microscope image of ice grain boundary and the distributions of reagents, which are represented by the Raman peak intensity. Note that the peaks were normalized because of the relatively high intensity of NO_3^- (1050 cm^{-1}) than the others. Experimental conditions: $[H_2O_2]_0$ = 40 mM; $[NO_2^-]_0$ = 20 mM; $[BA]_0$ = 1 mM; $[HCl]_0$ = 5 mM.

to the production of NO_3^- from the reaction. As we examined the system within 30 min, this result reveals that the reaction occurred rapidly in the concentrated region. In addition, if some portions of HONO and H_2O_2 were incorporated in ice crystals by their distribution characteristics in water, its effects were not significant on BA degradation. This was determined using the Raman microscope; we found that most of the species concentrated in the grain boundary region.

Characteristic of BA Oxidation via In Situ Generated Peroxynitrous Acid in Ice. Figure 4a,b shows the influence that the initial H_2O_2/NO_2^- ratio has on the BA decomposition in the aqueous and frozen systems. The initial H_2O_2 concentration was varied from 0.1 to 5 mM, and the initial NO_2^- concentration was varied from 0.1 to 1 mM. The overall enhancement of BA decomposition was observed in the frozen samples compared with the aqueous cases. However, the same or higher amount of NO_2^-, with respect to the amount of H_2O_2, inhibited the BA decomposition. Notably, the 1:1 H_2O_2/NO_2^- ratio did not significantly inhibit BA degradation at pH 3 in the aqueous system, while the 1:2 H_2O_2:NO_2^- ratio apparently inhibited BA degradation (Figure 4c). In fact, the initial BA concentration in our experiment was 0.02 mM; therefore, 1 mM NO_2^- was 50-fold higher than the BA concentration. Additionally, 0.1 mM H_2O_2 and NO_2^- (1:1 dosage ratio), which only represents a 5-fold higher NO_2^- concentration with respect to the BA concentration, in the frozen system led to the decomposition of ∼20% of BA (Figure 4b). These results suggest that NO_2^- competes with BA owing to the oxidative attack of HOONO. However, if this speculation is true, a high initial concentration of BA can be more effectively decomposed than a low initial concentration of BA. Figure 4d demonstrates the influence of the initial BA concentration in the frozen H_2O_2/NO_2^- system. The BA decomposition efficiency ($100 \times (1 - [BA]/[BA]_0)$; filled bar) decreased with an increase in the initial BA concentration; therefore, we questioned the possibility of the scavenging effect of NO_2^-. In contrast, when we compare the amount of decomposed BA with the BA dose, a positive relationship between them was established (empty bar). The 20 μM BA decomposed at an initial BA concentration of 100 μM, while only 10 μM BA was decomposed at an initial BA dosage of 20 μM. Based on this, we believe that the decline in the BA decomposition efficiency at high BA concentrations can be ascribed to the enhanced generation of byproducts that compete with BA; the scavenging effect of NO_2^- is an alternative scenario. Furthermore, the specific situation at the ice grain boundary should be considered to elucidate the inhibition via NO_2^- in the frozen system because freeze concentration occurred. When we observed the disappearance of HONO with reactant concentrations of 10 mM and 1 mM in the aqueous solution at a pH of 3, the fast reaction occurred in the concentrated case, i.e., the reaction was almost completed within 10 min at 10 mM, whereas the reaction lasted 60 min at 1 mM (Figure S7). Thus, we suggest that concentrated NO_2^- reacts with HOONO and rapidly transforms to NO_3^-, thereby regenerating NO_2^-:

$$NO_2^- + HOONO \rightarrow NO_3^- + HONO \quad (6)$$

$$HONO \leftrightarrow NO_2^- + H^+ (pK_a = 3.4) \quad (7)$$

Consequently, although NO_2^- was consumed by HOONO, a stoichiometric ratio of 1:1 between H_2O_2 and NO_2^- can be established owing to the resupply of NO_2^- (HONO reacts with H_2O_2) in this manner.

The reactivity of HOONO was estimated by testing the degradation of various benzene substituents in the frozen H_2O_2/NO_2^- system (Figure 5). Overall, the H_2O_2/NO_2^- cases showed observable reactivity, except in the terephthalic acid case, indicating the nonselective oxidative nature of HOONO. We suggest that the solubility of terephthalic acid (<15 mg/L) resulted in a low degradation efficiency in the ice because we observed 50% of terephthalic acid degradation in the aqueous H_2O_2/NO_2^- system at pH 3 (Figure S8). Although we showed

https://doi.org/10.1021/acs.est.1c05705
Environ. Sci. Technol. 2022, 56, 2323−2333

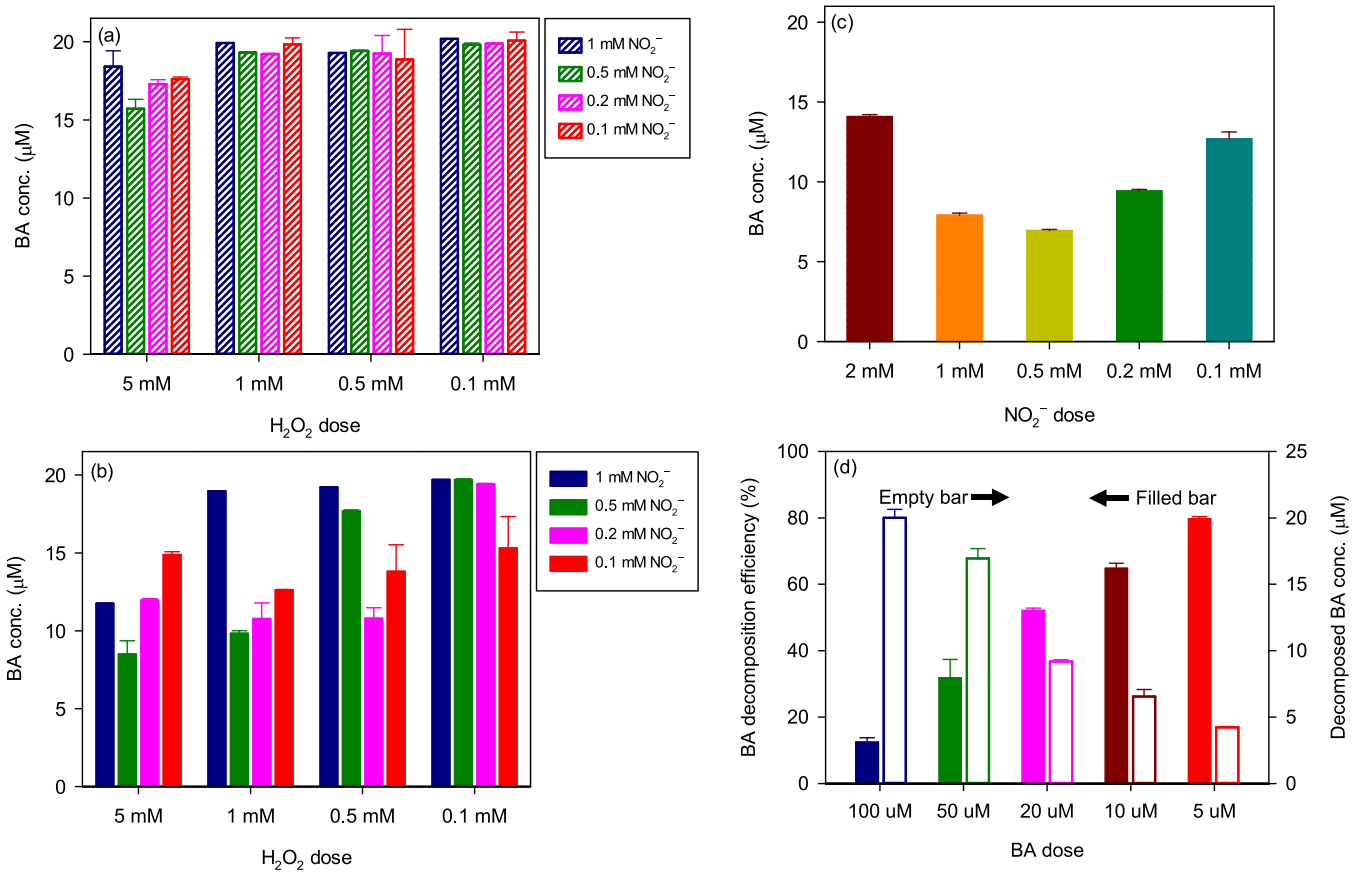

Figure 4. Influence of the initial H_2O_2/NO_2^- ratio on BA decomposition in (a) aqueous system and (b) frozen H_2O_2/NO_2^- system. Experimental conditions: $[BA]_0$ = 20 μM; pH_i = 4.0 (adjusted by $HClO_4$); reaction time = 1 h; temperature: frozen system (Fz.) = −20 °C, aqueous system (Aq.) = 25 °C. (c) Acidic aqueous system of pH 3. Experimental conditions: $[BA]_0$ = 20 μM; $[H_2O_2]_0$ = 1 mM; pH_i = 3.0 (adjusted by $HClO_4$); reaction time = 1 h. (d) Influence of the initial BA concentration on the BA decomposition in the frozen H_2O_2/NO_2^- system. Experimental conditions: $[H_2O_2]_0$ = 1 mM; $[NO_2^-]_0$ = 0.5 mM; pH_i = 4.0 (adjusted by $HClO_4$); reaction time = 1 h.

the nonselective reactivity of HOONO, its efficiency differed from that of benzene derivatives. Note that one of the reaction modes of HOONO may involve electrophilic substitution, and the electrophilic addition to the aromatic ring of the electrophile is negatively related to the Hammett constant. Accordingly, the degradation efficiencies of the substances in the frozen H_2O_2/NO_2^- system decreased with an increase in the electrophilic substituent constant σ^+ (Figure 5, top row[56,57]). This trend was also observed in the HONO system (i.e., the presence of only NO_2^-), but the HONO system was not appreciably reactive in other cases (Figure 5, middle and bottom rows). However, the degradation of substances in the frozen H_2O_2/NO_2^- system was also related to the Hammett constants σ^- and σ_p.[56−58] Although a decrease in chlorobenzene was observed, we speculate that this is occurred because of volatilization during freezing because chlorobenzene was also removed in the only-H_2O_2 case. However, the concentration of chlorobenzene was significantly lower in the case with H_2O_2/NO_2^-, showing the evident oxidation by HOONO.

Identification of Reaction Byproducts. The reaction of HOONO involves direct oxidation, nitration, and hydroxylation.[27−35] Accordingly, we can observe hydroxylated byproducts, as well as nitrated compounds and decarboxylated substrates. We first explored the byproducts of BA degradation. We then degraded some selected BA derivatives that were used as the starting compounds, namely, 4-nitrobenzoic acid (nitrated compound) and 2- and 4-hydroxybenzoic acid (hydroxylated compound), to compare the results with BA degradation and examine the reaction pathway. Hereafter, we refer to "the starting compounds" (it is a separated system; not byproducts in the BA system!) as their abbreviations, i.e., BZA (H_2O_2/benzoic acid/NO_2^- system; red), 2-HBA (H_2O_2/2-hydroxybenzoic acid/NO_2^- system; blue), 4-HBA (H_2O_2/4-hydroxybenzoic acid/NO_2^- system; green), and 4-NBA (H_2O_2/4-nitrobenzoic acid/NO_2^- system; yellow). Note that the signal in the BZA was amplified compared with the other starting compound system because the concentration of the other starting compounds was much higher (20 μM) than the BA oxidation products (~nM). Figure 6 shows the detected products in the starting compounds. Most importantly, we confirmed that the byproduct signals apparently derived from the examined reaction (note that we can exclude the signal not derived from the oxidation of HOONO, such as $HClO_4$, by comparison with the background signals).

Interestingly, in the BZA, the aqueous (gray line at the top row) system showed an intense 2-hydroxybenzoic acid signal ($[M - H]^-$ m/z 137.0235), which was comparable with that in the frozen system (red line), even though the degradation of BA was not significant. Additionally, the peaks of 3- and 4-hydroxybenzoic acid were identifiable in the aqueous system, but their intensities were lower than those in the frozen system. At this moment, we noted that the relative intensities of those three hydroxybenzoic acid isomers are not directly related to

https://doi.org/10.1021/acs.est.1c05705
Environ. Sci. Technol. 2022, 56, 2323−2333

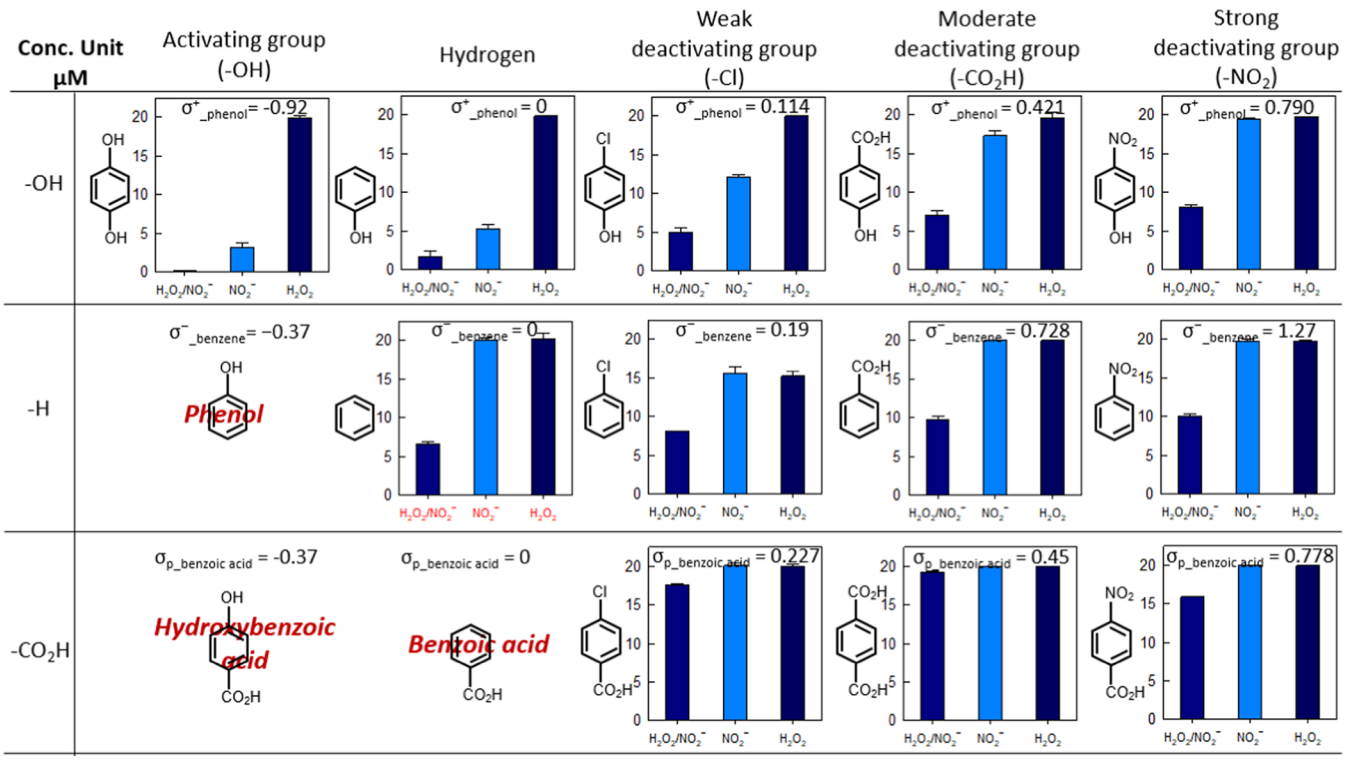

Figure 5. Oxidative degradation of various benzene derivatives in the frozen H_2O_2/NO_2^- system. Experimental conditions: $[Organics]_0$ = 20 μM; $[H_2O_2]_0$ = 1 mM; $[NO_2^-]_0$ = 0.5 mM; pH_i = 4.0; reaction time = 1 h. The Hammett constants were obtained from refs 56−58.

the concentration ratio: the ionization tendency affects the intensity (the estimated concentrations of salicylic acid and 4-hydroxybenzoic acid in the frozen system were ∼0.384 and 0.372 μM, respectively). Note that the aqueous system of pH 3 showed significant BA degradation (Figure 2), implying weakened reactivity in the H_2O_2/NO_2^- system at a high pH. Otherwise, we found no other intense signal under aqueous conditions comparable to the frozen system (Figure S9). Furthermore, the generation of nitrobenzoic acids was negligible in the aqueous solution (Figure 6; gray in the top-right) such that the nitration reactivity of HOONO was likely weaker than the hydroxylation reactivity under aqueous condition (pH 4). It is noted that the electrophilic substitution on the aromatic ring, which has deactivating group on it, prefer to attack the meta-position of the aromatic ring. Accordingly, we found that dominant 3-nitrobenzoic acid with respect to 4-nitrobenzoic acid. Furthermore, we found that BA degradation does not yield *para*-positioned dinitrobenzoic acid because there is no common peak position between BZA and 4-NBA (m/z 210.9994, middle row). Thus, the peak on the red line at 8.9 min of m/z 210.9994 likely represented 3,5-dinitrobenzoic acid.

The production of dihydroxybenzoic acid (m/z 153.0185) was also differentiated in the starting compounds. While BZA yielded three peaks, 4-HBA yielded only one peak at a retention time of 5.5 min and 2-HBA yielded two peaks at 6.4 and 7.1 min. Therefore, the compound at 5.5 min did not contain an *ortho*-positioned hydroxyl group, and the remaining compounds did not have a para-positioned one. A reasonable explanation for this is that the meta-hydroxylation of hydroxybenzoic acid mainly occurred. To compare the characteristics of the $^{\bullet}$OH-involved reaction, we employed the Fenton system and compared it with the H_2O_2/NO_2^- system (Figure S10). We found that the Fenton system also showed no common peak for dihydroxybenzoic acid at either 2-HBA or 4-HBA (Figure S10a). However, 2-HBA showed three peaks at the Fenton system, while the H_2O_2/NO_2^- system showed only two peaks at 2-HBA (both the frozen and acidic aqueous cases; Figure S10b). Hence, we assume that the −OH addition to the *ortho*-position is not negligible when $^{\bullet}$OH attacks 2-hydroxybenzoic acid, while HOONO showed no responsible signal according to this. Therefore, we speculate that the oxidation mechanism between HOONO and $^{\bullet}$OH is slightly different. Besides, based on the mono-hydroxylation of BA, both systems showed the apparent generation of 2-, 3-, and 4-hydroxybenzoic acid and the signal ratios among the isomers were slightly different (note that we matched the BA decomposition at 50% of its initial concentration; Figure S10c). Again, we emphasize that the intensity ratio does not directly indicate the concentration ratio; rather, it was reported that the *meta*-hydroxybenzoic acid yield by $^{\bullet}$OH was highest among the isomers.[59] In fact, although HOONO is not a radical oxidant, the H_2O_2/NO_2^- system was ineffective with the addition of the radical scavenging reagent methanol (Figure S11). We believe that further studies clarify the characteristic differences between HOONO and $^{\bullet}$OH.

The features of trihydroxybenzoic acid (m/z 169.0136) were difficult to explain because there were many spread peaks, and the peak intensity was low. We believe that the peaks with retention time >5 min were produced at the electrospray stage because they overlapped with their mother compounds, such as mono- and dihydroxybenzoic acid.[60] Similarly, the detected benzenediol peaks (m/z 109.0284), which have retention times >5 min, might be produced from the transformation of the mother compounds by corona discharge.[61] However, those hydrophilic compounds were assuredly generated because the evident signals were found at early retention times (<5 min;

https://doi.org/10.1021/acs.est.1c05705
Environ. Sci. Technol. 2022, 56, 2323−2333

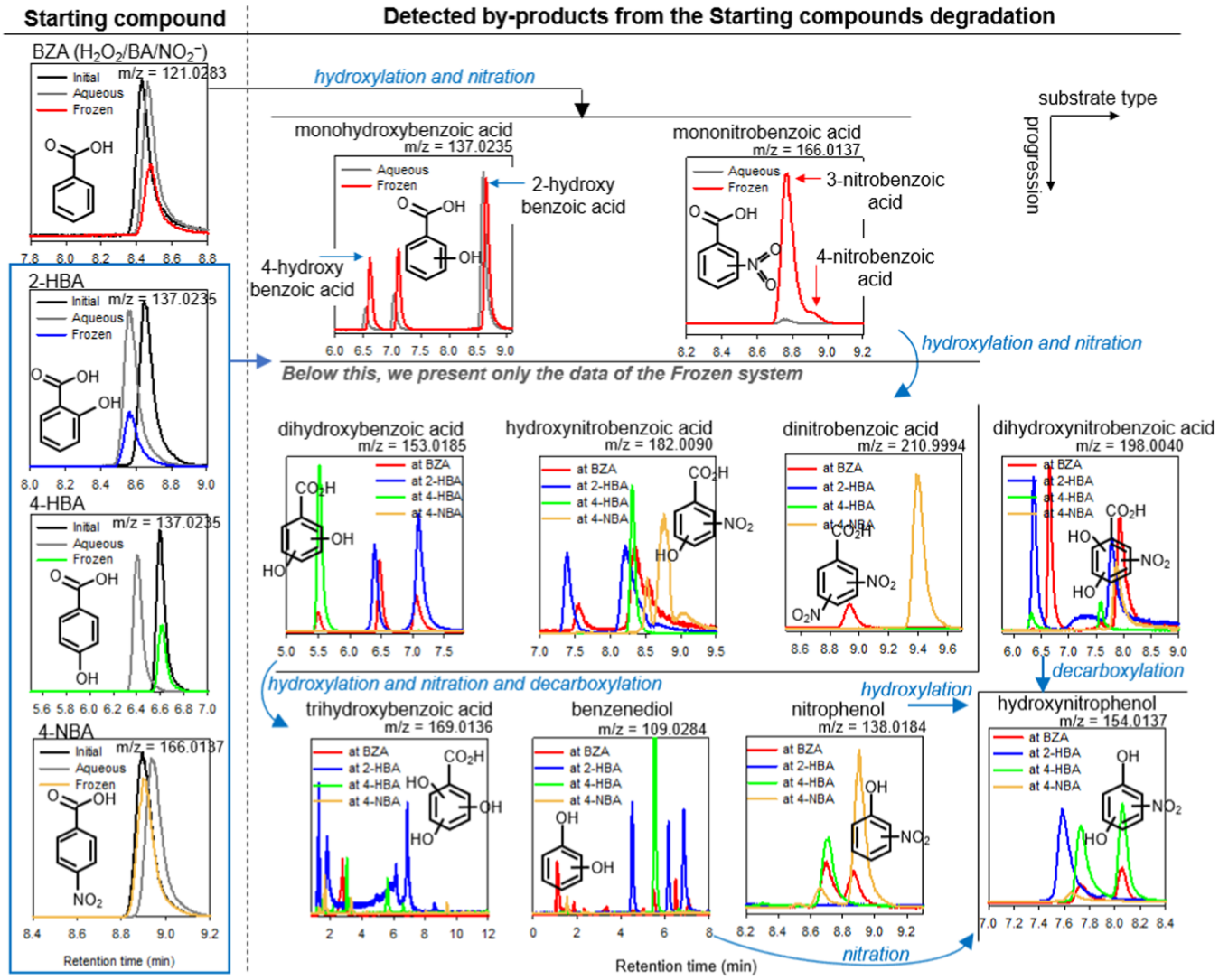

Figure 6. Detected degradation byproducts from LC-MS. Experimental conditions: $[Organics]_0$ = 20 μM; $[H_2O_2]_0$ = 1 mM; $[NO_2^-]_0$ = 0.5 mM; pH_i = 4.0 (adjusted by $HClO_4$); temperature: frozen system = −20 °C, aqueous system = 25 °C; reaction time = 1 h.

note that we confirmed that the catechol peak was positioned at 5 min).

Hydroxynitrobenzoic acid (m/z 182.0090) can be generated through two pathways: hydroxylation-first nitration-after, or vice versa. However, we propose that the former is more prone to occur than the latter because hydroxylated compounds are more easily decomposed than nitrated compounds, as illustrated in Figure 5. We found three peaks at 7.5, 8.4, and 8.6 min at BZA with m/z 182.0090. The earliest peak also appeared at 2-HBA, and because no peak was produced at this retention time in 4-NBA, this is likely 2-hydroxy-3-nitrobenzoic acid. The middle one (8.4 min) appeared at 2-HBA and 4-HBA both, so we suggest that the retention time of 2-hydroxy-5-nitrobenzoic acid is close to the retention time of 4-hydroxy-3-nitrobenzoic acid. From the comparison with 4-NBA, we suggest that 8.6 min is the retention time of 3-hydroxy-4-nitrobenzoic acid. Then, because hydroxylation increases the polarity of aromatic compounds, which results in the pulled retention time of m/z 198.0040 from the retention time of m/z 182.0090 in the C-18 column, we can confirm that dihydroxynitrobenzoic acid (m/z 198.0040) is without doubt generated.

We also suggest that decarboxylation can occur during oxidation. We found a clear signal of nitrophenol (m/z 138.0184) and hydroxynitrophenol (m/z 154.0137). The nitrophenol (bottom, third from left), at a position 8.7 min, was 4-nitrophenol because we confirmed its retention time via the comparison with a standard sample. 4-HBA showed one peak with respect to this such that decarboxylation occurred earlier than nitration. 2-HBA showed no peaks of nitrophenol such that the ortho-positioned hydroxyl group likely provided decarboxylation-resistant characteristics. The 8.9 min of m/z 138.0184 should be derived from the decarboxylation of 3-hydroxy-4-nitrobenzoic acid because there was no associated signal at 2-HBA and 4-HBA. Also, hydroxynitrophenol (m/z 154.0137) was likely mainly generated from the decarboxylation of dihydroxynitrobenzoic acid because the peaks were not well matched with the trend in m/z 138.0184 and m/z 109.0284 peaks. Hence, discussing the hydroxylation of nitrophenol and the nitration of benzenediol based on this result is difficult. If the decarboxylation occurred at the very early stage of oxidation, we could identify it, but our UHPLC/ESI/MS technique was not suitable to detect benzene and phenol (we think that the APPI ionization source is more

https://doi.org/10.1021/acs.est.1c05705
Environ. Sci. Technol. 2022, 56, 2323−2333

suitable for detecting the nonpolar benzene molecule than ESI).

Freezing-Induced BA Degradation by H_2O_2/NO_2^- System at Natural Imitated Environment. As mentioned in Figures 4 and 5, the interaction between BA and HOONO can be affected by other species, such as byproducts and nitrite. Generally, natural water contains many ingredients. As a result, BA degradation by the H_2O_2/NO_2^- system could be retarded in natural environments. Additionally, ice production in an ethanol bath is more efficient than in a refrigerator (air-cooling) because the heat transfer rates between the two media are different. Thus, to assess the impact of the real condition, we observed the BA degradation efficiency of the H_2O_2/NO_2^- system in an imitated natural environment using the air-cooling system and stream and rain waters (Figure 7). The

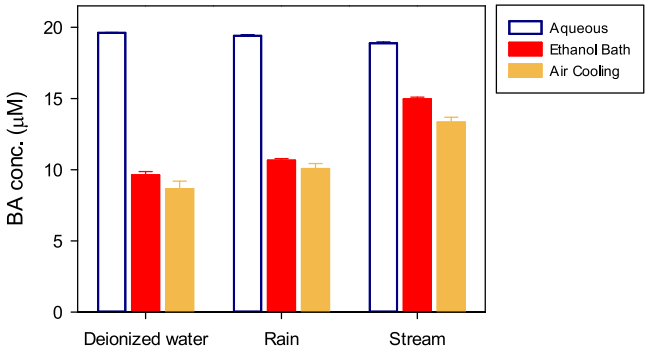

Figure 7. BA degradation by the H_2O_2/NO_2^- system at natural imitated environments. Experimental conditions: $[BA]_0$ = 20 μM; $[NO_2^-]_0$ = 0.5 mM; $[H_2O_2]_0$ = 1 mM; temperature: frozen system (Fz.) = −20 °C, aqueous system (Aq.) = 25 °C; reaction time = 2 h; pH = 4 (adjusted by $HClO_4$).

constituents under different water conditions are listed in Table S1 (note that we added 1 mM H_2O_2 and 0.5 mM NO_2^- in all waters and adjusted the initial pH of 4). Overall, the freezing method did not influence the BA degradation significantly. The difference between deionized water and rain was marginal, although the higher TOC with respect to the deionized water was measured in rainwater. Although the BA degradation in the stream water showed a retarded performance, the effect of freezing was also apparent in the stream. We believe that this retardation in the stream was derived from a higher concentration of species compared with the other two cases (Table S1).

Environmental Implications. The NO_2^- concentration varies depending on the situation: it is reported that about a few nM of nitrite presents at snow surface and droplet,[11,62] but it can increase up to about several hundred μM in fogwater[62,63] and significantly concentrated in the groundwater and municipal water due to industrial and agricultural activity.[64] Although H_2O_2 is not as stable as NO_2^-, H_2O_2 is also ubiquitous in aquatic environments: it can be produced by natural chemical reactions and biological processes.[65,66] The presence of H_2O_2 has been identified in various environments, including polar regions.[67−69] Freezing occurs globally on Earth. While freezing generally freezes the progression of chemical reactions, it can accelerate the reaction under specific situations because the water transforms its phase into ice and generates highly concentrated microreactors inside (freeze concentration effect). The chemistry of nitrite is associated with this unique reaction such that it can provide a highly oxidative environment for BA oxidation when it reacts with H_2O_2 under slightly acidic conditions. According to this, although the role of freezing has not been significantly considered for the transformation of aromatic compounds as carbon budget yet, it needed to be accounted for in environmental chemistry. Then, proxynitrie can also be generated from the reaction of N_3^-/O_3 and $^{\bullet}NO/O_2^{\bullet-}$; thus, we further study the effect of freezing on these systems.

HOONO is generally considered to be a strong nitration reagent. However, it is also a strong hydroxylation reagent. There are many arguments regarding the derivation of hydroxylation, such as the generation of $^{\bullet}OH$. Although we found a different reaction pathway between the H_2O_2/NO_2^- and the Fenton system, further studies are required to reveal the characteristics of HOONO.

■ ASSOCIATED CONTENT

Supporting Information

The Supporting Information is available free of charge at https://pubs.acs.org/doi/10.1021/acs.est.1c05705.

Chemical reagents used in this study (Text S1); estimation method of the pH in ice (Text S2); constituents in different water conditions (Table S1); concentration profiles of H_2O_2, NO_2^-, and NO_3^- in the frozen system (Figure S1); pH-dependent molar fraction of nitrite (Figure S2); BA degradation at the absence of hydrogen peroxide or nitrite in pH change (Figure S3); Arrhenius plot of nitrite decomposition under aqueous condition (Figure S4); BA degradation in the H_2O_2/NO_3^- system (Figure S5); BA transformation at various situations in the acidic aqueous system (Figure S6); UV−visible absorption spectra of the H_2O_2/NO_2^- system (Figure S7); degradation of terephthalic acid by the aqueous H_2O_2/NO_2^- system at pH 3 (Figure S8); BA degradation byproducts detected by LC-MS in the aqueous and frozen system (Figure S9); chromatogram of di-hydroxybenzoic acid on LC-MS (Figure S10); and effect of methanol in the frozen H_2O_2/NO_2^- system (Figure S11) (PDF)

■ AUTHOR INFORMATION

Corresponding Author

Kitae Kim − *Korea Polar Research Institute (KOPRI), Incheon 21990, Republic of Korea; Department of Polar Science, University of Science of Technology (UST), Incheon 21990, Republic of Korea;* orcid.org/0000-0003-0803-3547; Phone: +82-32-760-5365; Email: ktkim@kopri.re.kr; Fax: +82-32-760-5399

Authors

Yong-Yoon Ahn − *Korea Polar Research Institute (KOPRI), Incheon 21990, Republic of Korea*

Jungwon Kim − *Department of Environmental Sciences and Biotechnology, Hallym University, Chuncheon, Gangwon-do 24252, Republic of Korea;* orcid.org/0000-0001-7804-7587

Complete contact information is available at: https://pubs.acs.org/10.1021/acs.est.1c05705

Notes

The authors declare no competing financial interest.

https://doi.org/10.1021/acs.est.1c05705
Environ. Sci. Technol. 2022, 56, 2323−2333

■ ACKNOWLEDGMENTS

This research was supported by the Korea Polar Research Institute (KOPRI) project (PE21120) and was part of the project titled "Development of potential antibiotic compounds using polar organism resources (15250103, KOPRI Grant PM21030)", funded by the Ministry of Oceans and Fisheries, Korea.

■ REFERENCES

(1) Zhang, X.; Zhang, C.; Sun, X.; Yang, J.; Zhu, C. Mechanism and kinetic study of the reaction of benzoic acid with OH, NO3 and SO4− radicals in the atmosphere. *RSC Adv.* **2019**, *9*, 18971−18977.
(2) Min, D. W.; Kim, K.; Lui, K. H.; Kim, B.; Kim, S.; Cho, J.; Choi, W. Abiotic Formation of Humic-Like Substances through Freezing-Accelerated Reaction of Phenolic Compounds and Nitrite. *Environ. Sci. Technol.* **2019**, *53*, 7410−7418.
(3) Vione, D.; Maurino, V.; Minero, C.; Borghesi, D.; Lucchiari, M.; Pelizzetti, E. New Processes in the Environmental Chemistry of Nitrite. 2. The Role of Hydrogen Peroxide. *Environ. Sci. Technol.* **2003**, *37*, 4635−4641.
(4) Kroflič, A.; Huš, M.; Grilc, M.; Grgić, I. Underappreciated and Complex Role of Nitrous Acid in Aromatic Nitration under Mild Environmental Conditions: The Case of Activated Methoxyphenols. *Environ. Sci. Technol.* **2018**, *52*, 13756−13765.
(5) Vidović, K.; Lašič Jurković, D.; Šala, M.; Kroflič, A.; Grgić, I. Nighttime Aqueous-Phase Formation of Nitrocatechols in the Atmospheric Condensed Phase. *Environ. Sci. Technol.* **2018**, *52*, 9722−9730.
(6) Kroflič, A.; Grilc, M.; Grgić, I. Unraveling Pathways of Guaiacol Nitration in Atmospheric Waters: Nitrite, A Source of Reactive Nitronium Ion in the Atmosphere. *Environ. Sci. Technol.* **2015**, *49*, 9150−9158.
(7) Park, J. Y.; Lee, Y. N. Solubility and decomposition kinetics of nitrous acid in aqueous solution. *J. Phys. Chem. A* **1988**, *92*, 6294−6302.
(8) Kim, D.-h.; Lee, J.; Ryu, J.; Kim, K.; Choi, W. Arsenite Oxidation Initiated by the UV Photolysis of Nitrite and Nitrate. *Environ. Sci. Technol.* **2014**, *48*, 4030−4037.
(9) Zepp, R. G.; Hoigne, J.; Bader, H. Nitrate-induced photo-oxidation of trace organic chemicals in water. *Environ. Sci. Technol.* **1987**, *21*, 443−450.
(10) Riordan, E.; Minogue, N.; Healy, D.; O'Driscol, P.; Sodeau, J. R. Spectroscopic and Optimization Modeling Study of Nitrous Acid in Aqueous Solution. *J. Phys. Chem. A* **2005**, *109*, 779−786.
(11) Jacobi, H.-W.; Kleffmann, J.; Villena, G.; Wiesen, P.; King, M.; France, J.; Anastasio, C.; Staebler, R. Role of Nitrite in the Photochemical Formation of Radicals in the Snow. *Environ. Sci. Technol.* **2014**, *48*, 165−172.
(12) Takenaka, N.; Ueda, A.; Maeda, Y. Acceleration of the rate of nitrite oxidation by freezing in aqueous solution. *Nature* **1992**, *358*, 736−738.
(13) Takenaka, N.; Ueda, A.; Daimon, T.; Bandow, H.; Dohmaru, T.; Maeda, Y. Acceleration Mechanism of Chemical Reaction by Freezing: The Reaction of Nitrous Acid with Dissolved Oxygen. *J. Phys. Chem. B* **1996**, *100*, 13874−13884.
(14) Liu, X.; Huang, X.; Wu, Y.; Xu, Q.; Du, M.; Wang, D.; Yang, Q.; Liu, Y.; Ni, B.-J.; Yang, G.; Yang, F.; Wang, Q. Activation of nitrite by freezing process for anaerobic digestion enhancement of waste activated sludge: Performance and mechanisms. *Chem. Eng. J.* **2020**, *387*, No. 124147.
(15) Kim, K.; Ju, J.; Kim, B.; Chung, H. Y.; Vetráková, Lu.; Heger, D.; Saiz-Lopez, A.; Choi, W.; Kim, J. Nitrite-Induced Activation of Iodate into Molecular Iodine in Frozen Solution. *Environ. Sci. Technol.* **2019**, *53*, 4892−4900.
(16) Kim, K.; Chung, H. Y.; Ju, J.; Kim, J. Freezing-enhanced reduction of chromate by nitrite. *Sci. Total Environ.* **2017**, *590*−*591*, 107−113.
(17) Kim, K.; Kim, J.; Bokare, A. D.; Choi, W.; Yoon, H.-I.; Kim, J. Enhanced Removal of Hexavalent Chromium in the Presence of H2O2 in Frozen Aqueous Solutions. *Environ. Sci. Technol.* **2015**, *49*, 10937−10944.
(18) Robinson, C.; Boxe, C. S.; Guzmán, M. I.; Colussi, A. J.; Hoffmann, M. R. Acidity of Frozen Electrolyte Solutions. *J. Phys. Chem. B* **2006**, *110*, 7613−7616.
(19) Le, N. T. H.; Ju, J.; Kim, B.; Kim, M. S.; Lee, C.; Kim, S.; Choi, W.; Kim, K.; Kim, J. Freezing-enhanced non-radical oxidation of organic pollutants by peroxymonosulfate. *Chem. Eng. J.* **2020**, *388*, No. 124226.
(20) Choi, Y.; Yoon, H.-I.; Lee, C.; Vetráková, Lu.; Heger, D.; Kim, K.; Kim, J. Activation of Periodate by Freezing for the Degradation of Aqueous Organic Pollutants. *Environ. Sci. Technol.* **2018**, *52*, 5378−5385.
(21) Krausková, L'.; Procházková, J.; Klašková, M.; Filipová, L.; Chaloupková, R.; Malý, S.; Damborský, J.; Heger, D. Suppression of protein inactivation during freezing by minimizing pH changes using ionic cryoprotectants. *Int. J. Pharm.* **2016**, *509*, 41−49.
(22) Bronshteyn, V. L.; Chernov, A. Freezing potentials arising on solidification of dilute aqueous solutions of electrolytes. *J. Cryst. Growth* **1991**, *112*, 129−145.
(23) Imrichová, K.; Veselý, L.; Gasser, T. M.; Loerting, T.; Neděla, V.; Heger, D. Vitrification and increase of basicity in between ice Ih crystals in rapidly frozen dilute NaCl aqueous solutions. *J. Chem. Phys.* **2019**, *151*, No. 014503.
(24) Anastasio, C.; Chu, L. Photochemistry of Nitrous Acid (HONO) and Nitrous Acidium Ion (H2ONO+) in Aqueous Solution and Ice. *Environ. Sci. Technol.* **2009**, *43*, 1108−1114.
(25) Helaleh, M. I. H.; Korenaga, T. Fluorometric determination of nitrite with acetaminophen. *Microchem. J.* **2000**, *64*, 241−246.
(26) Vione, D.; Maurino, V.; Minero, C.; Pelizzetti, E. New Processes in the Environmental Chemistry of Nitrite: Nitration of Phenol upon Nitrite Photoinduced Oxidation. *Environ. Sci. Technol.* **2002**, *36*, 669−676.
(27) Beckman, J. S.; Koppenol, W. H. Nitric oxide, superoxide, and peroxynitrite: the good, the bad, and ugly. *Am. J. Physiol. Cell Physiol.* **1996**, *271*, C1424−C1437.
(28) Nonoyama, N.; Chiba, K.; Hisatome, K.; Suzuki, H.; Shintani, F. Nitration and hydroxylation of substituted phenols by peroxynitrite Kinetic feature and an alternative mechanistic view. *Tetrahedron Lett.* **1999**, *40*, 6933−6937.
(29) Coddington, J. W.; Hurst, J. K.; Lymar, S. V. Hydroxyl Radical Formation during Peroxynitrous Acid Decomposition. *J. Am. Chem. Soc.* **1999**, *121*, 2438−2443.
(30) Pou, S.; Nguyen, S. Y.; Gladwell, T.; Rosen, G. M. Does peroxynitrite generate hydroxyl radical? *Biochim. Biophys. Acta* **1995**, *1244*, 62−68.
(31) Uppu, R. M.; Squadrito, G. L.; Pryor, W. A. Acceleration of peroxynitrite oxidations by carbon dioxide. *Arch. Biochem. Biophys.* **1996**, *327*, 335−343.
(32) Lobachev, V.; Rudakov, E. Kinetics and Mechanism of the Oxidation of Alkanes and Alkenes with Peroxynitrous Acid in Aqueous Solution-Gas Phase Systems. *Kinet. Catal.* **2005**, *46*, 344−353.
(33) Vásquez-Vivar, J.; Santos, A. M.; Junqueira, V. B.; Augusto, O. Peroxynitrite-mediated formation of free radicals in human plasma: EPR detection of ascorbyl, albumin-thiyl and uric acid-derived free radicals. *Biochem. J.* **1996**, *314*, 869−876.
(34) Goldstein, S.; Merényi, G. The Chemistry of Peroxynitrite: Implications for Biological Activity. In *Methods Enzymology*; Academic Press, 2008; Chapter 4.
(35) Halfpenny, E.; Robinson, P. L. 168. Pernitrous acid. The reaction between hydrogen peroxide and nitrous acid, and the properties of an intermediate product. *J. Chem. Soc.* **1952**, 928−938.
(36) Hogg, N.; Darley-Usmar, V. M.; Wilson, M. T.; Moncada, S. Production of hydroxyl radicals from the simultaneous generation of superoxide and nitric oxide. *Biochem. J.* **1992**, *281*, 419−424.

https://doi.org/10.1021/acs.est.1c05705
Environ. Sci. Technol. 2022, 56, 2323−2333

(37) Kaur, H.; Whiteman, M.; Halliwell, B. Peroxynitrite-Dependent Aromatic Hydroxylation and Nitration of Salicylate and Phenylalanine. Is Hydroxyl Radical Involved? *Free Radical Res.* **1997**, *26*, 71−82.
(38) Kissner, R.; Nauser, T.; Kurz, C.; Koppenol, W. H. Peroxynitrous acid–where is the hydroxyl radical? *IUBMB Life* **2004**, *55*, 567−572.
(39) Koppenol, W. H.; Moreno, J. J.; Pryor, W. A.; Ischiropoulos, H.; Beckman, J. S. Peroxynitrite, a cloaked oxidant formed by nitric oxide and superoxide. *Chem. Res. Toxicol.* **1992**, *5*, 834−842.
(40) Kazakov, P.; Gorelenko, S.; Derevyagina, I.; Lukashov, O.; Mirzabekova, N. Oxidation of Substituted Toluenes by Nitric Acid. *Pharm. Chem. J.* **2020**, *54*, 46−48.
(41) Klassen, N. V.; Marchington, D.; McGowan, H. C. E. H2O2 Determination by the I3- Method and by KMnO4 Titration. *Anal. Chem.* **1994**, *66*, 2921−2925.
(42) Ohya, T.; Kanno, S. Formation of cyanide ion or cyanogen chloride through the cleavage of aromatic rings by nitrous acid or chlorine. XI: On the reaction of purine bases with hypochlorous acid in the presence of ammonium ion. *Chemosphere* **1989**, *19*, 1835−1842.
(43) Sun, F.; Xiao, Y.; Wu, D.; Zhu, W.; Zhou, Y. Nitrite-driven abiotic transformation of sulfonamide micropollutants during freezing process. *Chem. Eng. J.* **2017**, *327*, 1128−1134.
(44) Deborde, M.; von Gunten, U. Reactions of chlorine with inorganic and organic compounds during water treatment—Kinetics and mechanisms: A critical review. *Water Res.* **2008**, *42*, 13−51.
(45) Trifonow, I. Eigenschaften und Struktur der Persalpetersäure. *Z. Anorg. Allg. Chem.* **1922**, *124*, 123−135.
(46) Koppenol, H.; Peroxynitrite, W. *Detection in Biological Media: Challenges and Advances*; The Royal Society of Chemistry, 2016; Chapter 1.
(47) Ju, J.; Kim, J.; Vetráková, L'.; Seo, J.; Heger, D.; Lee, C.; Yoon, H.-I.; Kim, K.; Kim, J. Accelerated redox reaction between chromate and phenolic pollutants during freezing. *J. Hazard. Mater.* **2017**, *329*, 330−338.
(48) Han, T. U.; Kim, J.; Kim, K. Freezing-accelerated removal of chromate by biochar synthesized from waste rice husk. *Sep. Purif. Technol.* **2020**, *250*, No. 117233.
(49) Nguyen, Q. A.; Kim, B.; Chung, H. Y.; Kim, J.; Kim, K. Enhanced reduction of hexavalent chromium by hydrogen sulfide in frozen solution. *Sep. Purif. Technol.* **2020**, *251*, No. 117377.
(50) Heger, D.; Klánová, J.; Klán, P. Enhanced Protonation of Cresol Red in Acidic Aqueous Solutions Caused by Freezing. *J. Phys. Chem. B* **2006**, *110*, 1277−1287.
(51) Lee, D. H.; Kang, H. Proton Transport and Related Chemical Processes of Ice. *J. Phys. Chem. B* **2021**, *125*, 8270−8281.
(52) Takenaka, N.; Bandow, H. Chemical Kinetics of Reactions in the Unfrozen Solution of Ice. *J. Phys. Chem. A* **2007**, *111*, 8780−8786.
(53) Vacque, V.; Sombret, B.; Huvenne, J. P.; Legrand, P.; Suc, S. Characterisation of the O-O peroxide bond by vibrational spectroscopy. *Spectrochim. Acta, Part A* **1997**, *53*, 55−66.
(54) Irish, D. E.; Thorpe, R. V. Raman Spectral Studies of Cadmium−Nitrite Interactions in Aqueous Solutions and Crystals. *Can. J. Chem.* **1975**, *53*, 1414−1423.
(55) Gao, J.; Hu, Y.; Li, S.; Zhang, Y.; Chen, X. Adsorption of benzoic acid, phthalic acid on gold substrates studied by surface-enhanced Raman scattering spectroscopy and density functional theory calculations. *Spectrochim. Acta, Part A* **2013**, *104*, 41−47.
(56) Lee, Y.; Yoon, J.; von Gunten, U. Kinetics of the Oxidation of Phenols and Phenolic Endocrine Disruptors during Water Treatment with Ferrate (Fe(VI)). *Environ. Sci. Technol.* **2005**, *39*, 8978−8984.
(57) Leffler, J. E.; Grunwald, E. *Rates and Equilibria of Organic Reactions*; John Wiley & Sons, 1963; Chapter 7.
(58) Palusiak, M.; Domagała, M.; Dominikowska, J.; Bickelhaupt, F. M. The substituent effect on benzene dications. *Phys. Chem. Chem. Phys.* **2014**, *16*, 4752−4763.
(59) Klein, G. W.; Bhatia, K.; Madhavan, V.; Schuler, R. H. Reaction of hydroxyl radicals with benzoic acid. Isomer distribution in the radical intermediates. *J. Phys. Chem. C* **1975**, *79*, 1767−1774.
(60) Hassan, I.; Pavlov, J.; Errabelli, R.; Attygalle, A. B. Oxidative Ionization Under Certain Negative-Ion Mass Spectrometric Conditions. *J. Am. Soc. Mass Spectrom.* **2017**, *28*, 270−277.
(61) Pei, J.; Hsu, C.-C.; Wang, Y.; Yu, K. Corona discharge-induced reduction of quinones in negative electrospray ionization mass spectrometry. *RSC Adv.* **2017**, *7*, 43540−43545.
(62) Acker, K.; Beysens, D.; Möller, D. Nitrite in dew, fog, cloud and rain water: An indicator for heterogeneous processes on surfaces. *Atmos. Res.* **2008**, *87*, 200−212.
(63) Miller, D. R.; Byrd, J. E.; Perona, M. J. The source of Pb, Cu, and Zn in fogwater. *Water, Air, Soil Pollut.* **1987**, *32*, 329−340.
(64) Philips, S.; Laanbroek, H. J.; Verstraete, W. Origin, causes and effects of increased nitrite concentrations in aquatic environments. *Rev. Environ. Sci. Biotechnol.* **2002**, *1*, 115−141.
(65) Clark, C. D.; De Bruyn, W. J.; Jakubowski, S. D.; Grant, S. B. Hydrogen peroxide production in marine bathing waters: Implications for fecal indicator bacteria mortality. *Mar. Pollut. Bull.* **2008**, *56*, 397−401.
(66) Möller, D. Atmospheric hydrogen peroxide: Evidence for aqueous-phase formation from a historic perspective and a one-year measurement campaign. *Atmos. Environ.* **2009**, *43*, 5923−5936.
(67) Sakugawa, H.; Kaplan, I. R.; Tsai, W.; Cohen, Y. Atmospheric hydrogen peroxide. *Environ. Sci. Technol.* **1990**, *24*, 1452−1462.
(68) Neftel, A.; Jacob, P.; Klockow, D. Measurements of hydrogen peroxide in polar ice samples. *Nature* **1984**, *311*, 43−45.
(69) Kamiyama, K.; Motoyama, H.; Fujii, Y.; Watanabe, O. Distribution of hydrogen peroxide in surface snow over antarctic ice sheet. *Atmos. Environ.* **1996**, *30*, 967−972.

https://doi.org/10.1021/acs.est.1c05705
Environ. Sci. Technol. 2022, 56, 2323−2333